Syntheses and Cytotoxic Properties of the Curcumin Analogs 2,6-Bis(benzylidene)-4-phenylcyclohexanones

Ryan Davis[1], **Umashankar Das**[2], **Hilary Mackay**[1], **Toni Brown**[1], **Susan L. Mooberry**[3], **Jonathan R. Dimmock**[2], **Moses Lee**[1], and **Hari Pati**[2]

[1]Department of Chemistry, Hope College, Holland, MI, USA

[2]College of Pharmacy and Nutrition, University of Saskatchewan, Saskatoon, Saskatchewan, Canada

[3]Department of Physiology and Medicine, Southwest Foundation for Biomedical Research, San Antonio, TX, USA

Abstract

Fifteen curcumin analogs were synthesized and tested for *in-vitro* cytotoxicity towards B16 and L1210 murine cancer cell lines using an MTT assay. Significant activity was discovered for two analogs: **8** (B16 IC_{50} = 1.6 μM; L1210 IC_{50} = 0.35 μM) and **9** (B16 IC_{50} = 0.51 μM; L1210 IC_{50} = 1.2 μM). Several other analogs exhibited notable cytotoxicity. The data from quantitative structure-activity relationships suggest that large electron-withdrawing substituents placed in the *meta*-position of the arylidene aryl rings enhance potencies. Compounds **8** and **9** were found using a cell-based assay to have virtually no effects on microtubules at concentrations up to 40 μM. These results suggest that tubulin inhibition is not the principal mechanism by which the curcumin analogs act.

Keywords

B16; Curcumin analogs; L1210; Microtubules; Structure-activity relationships

Introduction

Curcumin (Fig. 1), a bis-α,β-unsaturated β-diketone found in the rhizomes of the herbaceous plant turmeric, has been extensively studied due to its biological effects, especially its anticancer properties. Curcumin has significant anti-proliferative effects towards various human cancer cell lines derived from prostate, large intestine, bone, and white blood cells [1–4]. In addition, curcumin has been shown to have a degree of tumor specificity, targeting malignant cells in preference to non-malignant cells [5] and it is effective at low micromolar concentrations [6].

The mechanisms by which curcumin acts to control malignant cell growth are varied, and have been proposed to be tissue-specific [6]. Cellular apoptosis is one of the main mechanisms that has been studied [7, 8]. Curcumin is also known to slow angiogenesis by blocking AP-1 [9] and is known to down-regulate the oncogene MDM2 in prostate cancer [10]. It has also been reported that cur-cumin can inhibit the polymerization of tubulin for spindle- fiber formation during mitotic cell division [11]. This is of particular interest to one of the author's laboratory, which has extensively studied the effects of combretasta-tin-A4 analogs, such as chalcones and diarylheterocycles, as mitotic inhibitors. Presumably, cytotoxicity is mediated, at least in part, by microtubule depolymerization and inhibition of tubulin polymerization [12–17].

The current study reports the synthesis of fifteen cur-cumin analogs **1**–**15** for evaluation as cytotoxins. These analogs replaced the diketone moiety of curcumin with a 4-phenylcyclohexanone moiety. Cyclohexanone analogs that lack the 4-phenyl group have recently been reported and they were discovered to have significant anti-angiogenic activity, measured by the inhibition of the growth of SVR endothelial cells in culture [18]. Substituted heterocyclic analogs of curcumin namely various 3,5-bis(benzylidene)-4-piperidones have also been reported and they were found to be active in inhibiting the growth of cancer cells in culture [19, 20]. From molecular modeling and X-ray crystallography studies, a relationship between the conformation of the diaryl moieties and cytotoxicity, as well as the Hammett constant σ, was reported [20].

In the present study, the hydroxyl and methoxy substituents present on the aryl rings in curcumin were retained and, in addition, other groups were introduced in order to examine the possible relationships between stereo-electronic and hydrophobic factors and cytotoxicity. The cytotoxicity studies on the compounds were performed with a 72 h continuous exposure MTT assay, using murine B16 (melanoma) and L1210 (leukemia) cell lines. Two of the most potent compounds, **8** and **9**, underwent further evaluation for effects on cellular microtubules.

Results and discussion

Chemistry

The curcumin analogs depicted in Table 1 were synthesized using an acid catalyzed aldol condensation of the appropriate aryl aldehyde with 4-phenylcyclohexanone (Scheme 1). The products were purified by recrystallization from ethanol and were obtained in yields of 45–80%. The structures were ascertained by IR, NMR, and mass spectrometry. Compounds **1** and **10** have been described previously but only their photophysical properties were studied [21].

Cytotoxic activity in murine cell lines

The cytotoxicity of curcumin analogs **1**–**9**, **11**–**15** was assessed in B16 (murine melanoma) and L1210 (murine leukemia) cell lines using a 72 h continuous exposure MTT assay as previously described [14]. The concentration at which 50% cell growth was inhibited (IC$_{50}$, μM) was determined for each compound in triplicate experiments. Data could not be

obtained for compound **10** because it was insoluble in different solvents including dimethylsulfoxide. The results from the cytotoxicity studies are presented in Table 1.

The following general observations were made. First, the IC_{50} values of a number of the compounds are in the low micromolar range (1–10 μM) in 61% of the bioassays. In addition, the IC_{50} figures of both **8** and **9** in one of the bioassays are sub-micromolar and they are clearly lead molecules. Second, with the exception of **1**, the IC_{50} values of the compounds are similar in both screens.

Specifically, the following comparisons were made in attempting to discern correlations between the nature of the aryl substituents and cytotoxic potencies. First, the mode of action of conjugated unsaturated ketones includes alkylation of cellular thiols [22]. Hence, the electronic nature of the aryl substituents will affect the charge densities on the olefinic carbon atoms, which, in turn, will control the rate and extent of thiol alkylation. Linear and semilogarithmic plots were made between the Hammett s and Taft σ* values (Table 2) of the aryl substituents and the IC_{50} values which were less than 100 μM in the B16 assay. A trend towards a negative correlation was noted in the linear plot ($p = 0.083$). The analyses were repeated using the biological data in the L1210 screen, which indicated a negative correlation in the semilogarithmic plot ($p = 0.060$) and a linear plot ($p = 0.117$). Thus, cytotoxic potencies rise as the electron-withdrawing capacity of the aryl substituents increases. This observation is in accord with the view that a mode of action of these compounds is likely by reaction with cellular thiols.

Second, the hydrophobic and steric properties of aryl substituents can influence the magnitude of biological responses [23]. Linear and semilogarithmic plots were constructed between the IC_{50} values of **1**, **2**, **4** – **9**, and **12** – **14** in the B16 screen and both the Hansch π and molar refractivity (MR) values (Table 2). The process was repeated using the biological data for **2**, **4**–**9**, and **12**–**14** in the L1210 assay. No correlations were noted ($p > 0.05$), although a trend towards a negative correlation was observed in the semilogarithmic plot between the IC_{50} values in the B16 screen and the MR figures ($p = 0.089$). This observation suggests that potency is enhanced by increasing the size of the aryl substituents. A further steric feature of these molecules, which could influence cytotoxic potencies are the torsion angles θ_1 and θ_2 between the aryl rings and the adjacent olefinic linkages. Consequently, models of **1**, **2**, **4**–**9**, and **12**–**14** were built and the θ_1 and θ_2 angles recorded. Linear and semilogarithmic plots between the θ_1 and θ_2 values of these compounds and the IC_{50} figures in the B16 screen were made. The process was repeated using the data from the L1210 test except **1** was omitted (IC_{50} value of > 100 μM). No correlations were observed ($p > 0.05$). Thus, these torsion angles are unlikely to exert a major influence on cytotoxic potencies. Models revealed that the locations of the methoxy group of **7** and the 3-methoxy substituent of **9** virtually overlapped (Fig. 2) which may explain the significant potencies of both compounds. In addition, since the IC_{50} values of **1** are greater than **2**, the 4-methoxy group lowers cytotoxic potencies. Figure 2 reveals that the 4-methoxy substituents of **1** and **9** are in similar locations, suggesting that this group in **9** has an adverse effect on potency and that the 3,5-dimethoxy analog may well exceed the potencies of **9**.

Third, the positions of the substituents on the benzylidene aryl rings in relation to cytotoxic potencies were addressed. A review of the IC_{50} values for compounds which possess a single *para* substituent namely **1**, **3**, **5**, **6**, **8** indicates that those molecules with electron-withdrawing groups (**5**, **6**, **8**) are more potent than the analogs with electron-repelling substituents (**1**, **3**). This observation confirms that in developing the cluster of unsaturated ketones, strongly electron-attracting groups should be attached to the benzylidene aryl rings. The *meta* position appears to be optimal for the methoxy group. Thus, the potency of **7** which possesses a single *meta*-methoxy substituent is greater than **1** having a single *para*-methoxy group. The addition of a 4-hydroxy moiety to **7** led to **14**, which has similar IC_{50} values as **7**. The number of *meta*-methoxy groups was increased in **9** which possesses high potency. On the other hand, placing methoxy groups in the *ortho* position as in **11** eliminates significant cytotoxic potency. The possibility that the *meta* position may be the optimal location was enhanced by the fact that the 3-bromo analog **12** had the lowest IC_{50} values apart from the lead compounds **8** and **9**. One may note, however, that the size of the group in the *meta* position is a consideration since the placing of the bulky 3-phenoxy substituent into **6** leading to **15** led to a marked reduction in potency. In summary, the available evidence in regard to structure-activity relationships in this series of compounds reveals that in general (i) the compounds are potent cytotoxins, (ii) large electron-withdrawing groups should be placed in the benzylidene aryl rings, and (iii) the *meta* position is likely the preferred location in producing analogs with low IC_{50} values.

Effects on cellular microtubules

Since curcumins have been reported to cause microtubule depolymerization and inhibit tubulin polymerization and angiogenesis, the effects of the two active compounds **8** and **9** on cellular microtubules were investigated [15, 24]. Results from these studies showed that compounds **8** and **9** were virtually inactive at concentrations up to 40 μM. These results suggest that the mechanism of cytotoxicity is unrelated to the disruption of microtubules.

Conclusion

The results from this study confirm that readily accessible curcumin analogs are potential cytotoxins for anti-cancer-drug discovery. It is concluded that large electron-withdrawing groups at the *meta* positions enhance cytotoxic potencies.

Experimental

Chemistry

All fifteen analogs were synthesized according to the following general procedure. Aqueous hydrochloric acid (35%, 0.5 mL) was added dropwise to a solution of 4-phenylcyclohexanone (500 mg) and the appropriate aryl aldehyde (2 equivalents) in ethanol (20 mL) at room temperature. The reaction mixture was stirred under reflux for 3–4 h monitoring by silica gel TLC plates (hexane/ethyl acetate, 9 : 1). The precipitate formed upon cooling to room temperature was filtered, washed with chilled ethanol, and recrystallized from ethanol (with the exception of **15** which was purified over silica eluting

with ethyl acetate/hexane, 5 : 95). The isolated chemical yields were between 70–80%, except compound **8** was isolated in 45% yield.

2,6-Bis[(4-methoxyphenyl)methinyl]-4-phenylcyclohexanone 1—Yellow solid. M.p. 1150C. ^{1}H-NMR (CDCl$_3$, 400 MHz): δ (ppm) = 2.98 (m, 3H), 3.28 (m, 2H), 3.81 (s, 6H), 6.88 (d, 4H, J = 8.8 Hz), 7.25–7.37 (m, 5H), 7.42 (d, 4H, J = 8.8 Hz), 7.83 (s, 2H). IR (KBr pellets cm^{-1}) ν = 3029, 2954, 2904, 2836, 2042, 1663, 1599, 1509, 1460, 1254, 1175, 1030, 988, 833, 703. ESI(APCI)-MS: m/z = 411 [M + 1].

2,6-bis(phenylmethinyl)-4-phenylcyclohexanone 2—Yellow solid. M.p. 132°C. ^{1}H-NMR (CDCl$_3$, 400 MHz): δ (ppm) = 2.99 (m, 3H), 3.29 (m, 2H), 7.26–7.45 (m, 15H), 7.87 (s, 2H). IR (KBr pellets cm^{-1}) ν = 3054, 3026, 2881, 1961, 1816, 1659, 1603, 1566, 1493, 1446, 1294, 1235, 1189, 1159, 986, 935, 762, 697. ESI(APCI)-MS: m/z = 351 [M + 1].

2,6-Bis[(4-methylphenyl)methinyl]-4-phenylcyclohexanone 3—Yellow solid. M.p. 1890C. ^{1}H-NMR (CDCl$_3$, 400 MHz): δ (ppm) =2.35 (s, 6H), 2.98 (m, 3H), 3.27 (m, 2H), 7.16 (d, 4H, J = 8.0 Hz), 7.23–7.36 (m, 9H), 7.84 (s, 2H). IR (KBr pellets cm^{-1}) ν = 3026, 2919, 2732, 1917, 1661, 1599, 1563, 1510, 1316, 1291, 1239, 1179, 1149, 989, 818, 750, 700. ESI(APCI)-MS: m/z = 379 [M + 1].

2,6-Bis[(3,4-methylenedioxyphenyl)methinyl]-4-phenylcyclohexanone 4— Yellow solid. M.p. 196°C. ^{1}H-NMR (CDCl$_3$, 400 MHz): δ (ppm) = 2.96 (m, 3H), 3.25 (m, 2H), 5.97 (s, 4H), 6.81 (d, 2H, J = 8.0 Hz), 6.94–6.99 (m, 4H), 7.25–7.37 (m, 5H), 7.77 (s, 2H). IR (KBr pellets cm^{-1}) ν = 3076, 3003, 2896, 2778, 1855, 1657, 1589, 1556, 1500, 1435, 1359, 1336, 1293, 1224, 1146, 1096, 1039, 989, 934, 867, 814, 759. ESI(APCI)-MS: m/z = 439 [M + 1].

2,6-Bis[(4-chlorophenyl)methinyl]-4-phenylcyclohexanone 5—Yellow solid. M.p. 171°C. ^{1}H-NMR (CDCl$_3$, 400 MHz): δ (ppm) = 2.97 (m, 3H), 3.22 (m, 2H), 7.25–7.28 (m, 4H), 7.33–7.38 (m, 9H), 7.80(s, 2H). IR (KBr pellets cm^{-1}) ν = 3064, 3028, 2899, 2564, 1911, 1666, 1604, 1490, 1407, 1309, 1281, 1237, 1185, 1146, 1094, 1011, 989, 833, 762, 698. ESI(APCI)-MS: m/z = 419 [M + 1].

2,6-Bis[(4-fluorophenyl)methinyl]-4-phenylcyclohexanone 6—Yellow solid. M.p. 159°C. ^{1}H-NMR (CDCl$_3$, 400 MHz): δ (ppm) = 2.96 (m, 3H), 3.22 (m, 2H), 7.02–7.06 (m, 4H), 7.24–7.35 (m, 5H), 7.39 (m, 4H), 7.81 (s, 2H). IR (KBr pellets cm^{-1}) ν = 3043, 2899, 2838, 1946, 1666, 1600, 1566, 1508, 1414, 1292, 1232, 1187, 1148, 1101, 989, 832, 754, 702. ESI(APCI)-MS: m/z = 387 [M + 1].

2,6-Bis[(3-methoxyphenyl)methinyl]-4-phenylcyclohexanone 7—Yellow solid. M.p. 97°C. ^{1}H-NMR (CDCl$_3$, 400 MHz): δ (ppm) = 2.96 (m, 3H), 3.27 (m, 2H), 3.78 (s, 6H), 6.83 (m, 2H), 6.94 (s, 2H), 7.00(m, 2H), 7.21–7.33 (m, 7H), 7.81 (s, 2H). IR (KBr pellets cm^{-1}) ν = 3068, 3017, 2952, 2891, 2837, 2577, 1938, 1660, 1601, 1575, 1481, 1433, 1246, 1196, 1215, 1157, 1051, 947, 899, 785, 743, 695. ESI(APCI)-MS: m/z = 411 [M + 1].

2,6-Bis[(4-nitrophenyl)methinyl]-4-phenylcyclohexanone 8—Yellow solid. M.p. 81°C. ^{1}H-NMR (CDCl$_3$, 400 MHz): δ (ppm) = 3.04 (m, 3H), 3.22 (m, 2H), 7.24–7.37 (m, 5H), 7.56 (d, 4H, J = 8.4 Hz), 7.87 (s, 2H), 8.22 (d, 4H, J = 8.8 Hz). IR (KBr pellets cm^{-1}) ν = 3070, 2924, 2847, 2447, 1935, 1665, 1594, 1518, 1345, 1300, 1240, 1192, 1152, 1110, 995, 908, 855, 761. ESI(APCI)-MS: m/z = 439 [M − 1].

2,6-Bis[(3,4,5-trimethoxyphenyl)methinyl]-4-phenylcyclohexanone 9—Yellow solid. M.p. 183°C. ^{1}H-NMR (CDCl$_3$, 400 MHz): δ (ppm) = 3.03 (m, 3H), 3.33 (m, 2H), 3.85 (s, 12H), 3.88 (s, 6H), 6.69 (s, 4H), 7.26–7.35 (m, 5H), 7.81 (s, 2H). IR (KBr pellets cm^{-1}) ν = 2995, 2941, 2838, 2000, 1657, 1578, 1503, 1454, 1417, 1346, 1286, 1243, 1127, 1020, 936, 836, 733. ESI(APCI)-MS: m/z = 531 [M + 1].

2,6-Bis[(4-dimethylaminophenyl)methinyl]-4-phenylcyclohexanone 10—Orange solid. M.p. 70°C. ^{1}H-NMR (CDCl$_3$, 400 MHz): δ (ppm) = 2.99 (m, 15H), 3.31 (m, 2H), 6.66 (d, 4H, J = 8.8Hz), 7.24–7.35 (m, 5H), 7.41 (d, 4H, J = 8.8 Hz), 7.83 (s, 2H); IR (KBr pellets cm^{-1}) ν = 3027, 2892, 2812, 2530, 1883, 1651, 1586, 1522, 1444, 1367, 1300, 1230, 1168, 1066, 988, 945, 818. ESI(APCI)-MS: m/z = 437 [M + 1].

2,6-Bis[(2,6-dimethoxyphenyl)methinyl]-4-phenylcyclohexanone 11—Yellow solid. M.p. 210°C. ^{1}H-NMR (CDCl$_3$, 400 MHz): δ (ppm) = 2.62 (m, 4H), 2.97 (m, 1H), 3.79 (s, 12H), 6.51 (d, 4H, J = 8.4 Hz), 7.13–7.25 (m, 7H), 7.73 (s, 2H). IR (KBr pellets cm^{-1}) ν = 2997, 2937, 2837, 2531, 1910, 1671, 1615, 1582, 1469, 1433, 1294, 1254, 1138, 1107, 1033, 988 761. ESI(APCI)-MS: m/z = 471 [M + 1].

2,6-Bis[(3-bromophenyl)methinyl]-4-phenylcyclohexanone 12—Yellow solid. M.p. 171°C. ^{1}H-NMR (CDCl$_3$, 400 MHz): δ (ppm) = 2.98 (m, 3H), 3.21 (m, 2H), 7.22–7.45 (m, 11H), 7.54 (s, 2H), 7.76 (s, 2H). IR (KBr pellets cm^{-1}) ν = 3056, 3027, 2908, 1947, 1745, 1662, 1605, 1574, 1475, 1411, 1286, 1239, 1188, 1153, 1103, 994, 788, 763. ESI(APCI)-MS: m/z = 506 [M + 1].

2,6-Bis[(2-chlorophenyl)methinyl]-4-phenylcyclohexanone 13—Yellow solid. M.p. 164°C. ^{1}H-NMR (CDCl$_3$, 400 MHz): δ (ppm) = 2.86–3.11 (m, 5H), 7.20–7.32 (m, 11H), 7.41–7.43 (m, 2H), 7.98 (s, 2H). IR (KBr pellets cm^{-1}) ν = 3060, 3026, 2870, 1960, 1812, 1671, 1609, 1587, 1467, 1436, 1295, 1230, 1189, 1150, 1047, 989, 919, 867, 760, 701. ESI(APCI)-MS: m/z = 419 [M + 1].

2,6-Bis[(3-hydroxy-4-methoxyphenyl)methinyl]-4-phenylcyclohexanone 14—Yellow solid. M.p. 161°C. ^{1}H-NMR (CDCl$_3$, 400 MHz): δ (ppm) = 2.99 (m, 3H), 3.29 (m, 2H), 3.88 (s, 6H), 5.78 (s, 2H), 6.89 (d, 2H, J = 8.4 Hz), 6.96 (d, 2H, J = 1.6 Hz), 7.04 (m, 2H), 7.24–7.36 (m, 5H), 7.80 (s, 2H). IR (KBr pellets cm^{-1}) ν = 3525, 3209, 2928, 1641, 1579, 1514, 1422, 1250, 1166, 1126, 1035, 1007, 936, 911, 856, 819. ESI(APCI)-MS: m/z = 443 [M + 1].

2,6-Bis[(4-fluoro-3-phenoxyphenyl)methinyl]-4-phenylcyclohexanone 15—Yellow semisolid. ^{1}H-NMR (CDCl$_3$, 400 MHz) δ (ppm) = 2.77 (m, 3H), 3.10 (m, 2H), 6.95–7.35 (m, 21H), 7.69 (s, 2H). IR (KBr pellets) ν = 3030, 2928, 2854, 1943, 1741, 1670,

1586, 1508, 1418, 1271, 1211, 1149, 1117, 1003, 818, 752, 694. ESI(APCI)-MS: m/z = 571 [M + 1].

Statistical analyses

The Hammett s values were taken from the literature [25] and the Taft σ^* figure has been reported previously [26]. The Hansch π and molar refractivity (MR) figures were obtained from published data [27]. The MR value of hydrogen is 1.03. Hence, in order that the relative bulk of the substituents was compared accurately, this figure was added to the MR value of the two groups in disubstituted compounds and 2.06 (2×1.03) for the monosubstituted analogs. The MR value for the unsubstituted compound **2** is 3.09. The linear and semilogarithmic plots were made using a commercial software package [28].

Molecular modeling

Models of **1,2,4–9**, and **12–14** were built using BioMedCache 6.1 for Windows [29]. The lowest energy conformations were obtained from optimized geometry calculations in MOPAC using AM1 parameters. The torsion angles for these compounds are as follows **1**: 46.7, −42.1; **2**: 48.7, −44.6; **4**: 49.0, −45.6; **5**: 51.0, −44.5; **6**: 48.7, −44.1; **7**: 47.4, −48.0; **8**: 49.5, −45.2; **9**: 53.4, −45.7; **12**: 47.8, −46.5; **13**: 92.9, −50.4 and **14**: 48.3, −45.6. Energy minimized structures of **1**, **7** and **9** were superimposed (the five carbon atoms, C=C-C-C=C) and are depicted in Fig. 2.

Biology

Curcumin analogs **1–15** were subjected to a continuous exposure 72 h MTT assay as described previously [14]. L1210 and B16 cell lines were purchased from ATCC (Manassas, VA, USA) and were maintained as previously reported [14]. The microtubule disrupting effects were evaluated in A-10 cells by indirect immunofluorescent techniques as previously described [24].

Acknowledgments

References

1. Chen AP, Xu J. Am J Physiol. 2005; 288:G447–G456.

2. Dorai T, Gehani N, Katz A. Prostate Cancer Prostatic Dis. 2000; 3:84–93. [PubMed: 12497104]

3. Kuo ML, Huang TS, Lin JK. Biochim Biophys Acta. 1996; 1317:95–100. [PubMed: 8950193]

4. Ozaki K, Kawata Y, Amano S, Hanazawa S. Biochem Pharmacol. 2000; 59:1577–1581. [PubMed: 10799655]

5. Plummer S, Wakelin D, Bouer M. Br J Cancer. 2000; 83(Suppl 1):20.

6. Sharma RA, Gescher AJ, Steward WP. Eur J Cancer. 2005; 41:1955–1968. [PubMed: 16081279]

7. Aggarwal BB, Kumar A, Bharti AC. Anticancer Res. 2003; 23:363–398. [PubMed: 12680238]

8. Tsvetkov P, Asher G, Reiss V, Shaul Y, et al. Proc Natl Acad Sci USA. 2005; 102:5535–5540. [PubMed: 15809436]

9. Huang TS, Lee SC, Lin JK. Proc Natl Acad Sci USA. 1991; 88:5292–5296. [PubMed: 1905019]

10. Li M, Zhang Z, Hill DL, Wang H, Zhang R. Cancer Res. 2007; 67:1988–1996. [PubMed: 17332326]

11. Gupta KK, Bharne SS, Rathinasamy K, Naik NR, Panda D. FEBS J. 2006; 273:5320–5332. [PubMed: 17069615]

12. Pati HN, Holt HL, LeBlanc R, Dickson J, et al. Med Chem Res. 2005; 14:19–25.Pati HN, Wicks M, Holt HL, LeBlanc R, et al. Heterocyclic Commun. 2005; 11:117–120.

13. Holt HL Jr, LeBlanc R, Dickson J, Brown T, et al. Heterocyclic Commun. 2005; 11:465–470.

14. LeBlanc R, Dickson J, Brown T, Stewart M, et al. Bioorg Med Chem. 2005; 13:6025–6034. [PubMed: 16055334]

15. Ruprich J, Prout A, Dickson J, Younglove B, et al. Lett Drug Des Discov. 2007; 4:144–148.

16. Johnson M, Younglove B, Lee L, LeBlanc R, et al. Bioorg Med Chem Lett. 2007; 17:5897–5901. [PubMed: 17827004]

17. Lee L, Davis R, Vanderham J, Hills P, et al. Eur J Med Chem. 2008 in press.

18. Robinson TP, Ehlers T, Hubbard RB, Bai XH, et al. Bioorg Med Chem Lett. 2003; 13:115–117. [PubMed: 12467629]

19. Dimmock JR, Padmanilayam MP, Puthucode RN, Nazarali AJ, et al. J Med Chem. 2001; 44:586–593. [PubMed: 11170648]

20. Dimmock JR, Jha A, Zello GA, Quail JW, et al. Eur J Med Chem. 2002; 37:961–972. [PubMed: 12660021]

21. Badaeva A, Timoteera TV, Masunov A, Tretiak S. J Phys Chem A. 2005; 109:7276–7284. [PubMed: 16834093]

22. Pati HN, Das U, Sharma RK, Dimmock JR. Mini Rev Med Chem. 2007; 7:131–139. [PubMed: 17305587]

23. Thomas, G. Medicinal Chemistry An Introduction. Vol. 50–54. John Wiley and Sons, Ltd; Chichester: 2000. p. 57-59.

24. Kong Y, Grembecka J, Edler MC, Hamel E, et al. ACS Chem Biol. 2005; 12:1007–1014.

25. Perrin, DD., Dempsey, B., Serjeant, EP. pKa Prediction for Organic Acids and Bases. Chapman and Hall; London: 1981. p. 109-112.p. 120

26. Taft, RW, Jr. Steric Effects in Organic Chemistry. Newman, MS., editor. John Wiley and Sons, Inc; New York: 1956. p. 591

27. Hansch, C., Leo, AJ. Substituent Constants for Correlation Analysis in Chemistry and Biology. John Wiley and Sons; New York: 1979. p. 49p. 84

28. Statistical Package for Social Sciences, SPSS for Windows, Standard Version, release 13.0. Chicago: SPSS Inc; 2004.

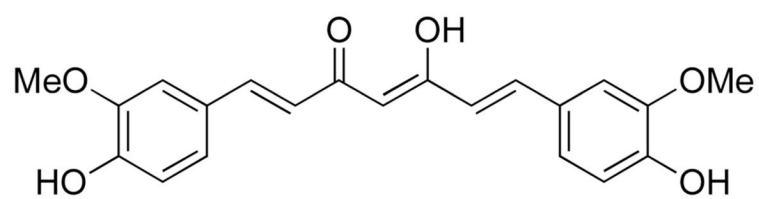29. BioMedCache 6.1 Windows, BioMedCache. Fujitsu America, Inc; 2003.
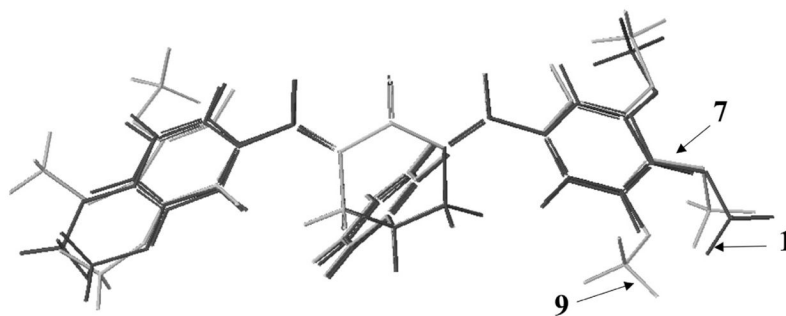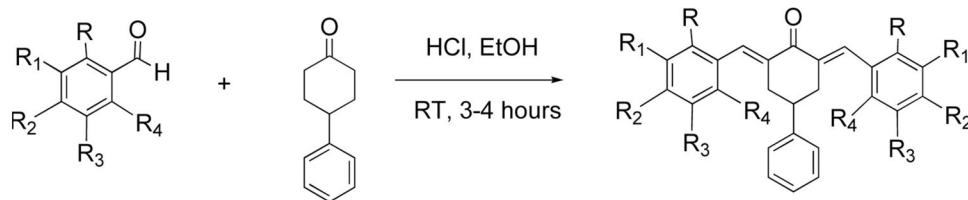
Figure 1.
Structure of curcumin.

Figure 2.
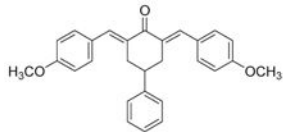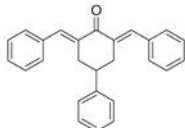Superimposed structures of **1**, **7**, and **9**.

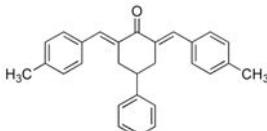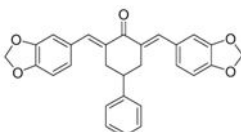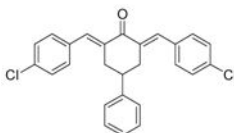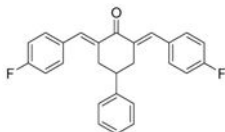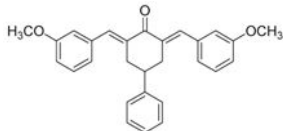**1**, R_2 = -OCH$_3$, R=R$_1$=R$_3$=R$_4$=H; **2**, R=R$_1$=R$_2$=R$_3$=R$_4$=H
3, R_2 = -CH$_3$, R=R$_1$=R$_3$=R$_4$=H; **4**, R$_1$-R$_2$ = -O-CH$_2$-O-, R=R$_3$=R$_4$=H
5, R_2 = -Cl, R=R$_1$=R$_3$=R$_4$=H; **6**, R$_2$ = -F, R=R$_1$=R$_3$=R$_4$=H
7, R_1 =-OCH$_3$, R=R$_2$=R$_3$=R$_4$=H; **8**, R$_2$ = -NO$_2$, R=R$_1$=R$_3$=R$_4$=H
9, R$_1$= R$_2$ = R$_3$ =-OCH$_3$, R= R$_4$=H; **10**, R$_2$ = -N(CH$_3$)$_2$, R=R$_1$=R$_3$=R$_4$=H
11, R= R$_4$= -OCH$_3$, R$_1$=R$_2$ =R$_3$ =H; **12**, R$_1$ =-Br , R=R$_2$=R$_3$=R$_4$=H
13, R= -Cl, R$_1$=R$_2$ =R$_3$=R$_4$=H; **14**, R$_1$ =-OCH$_3$, R$_2$= -OH, R=R$_3$=R$_4$=H
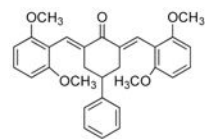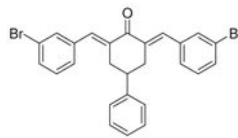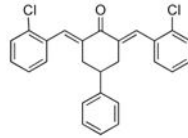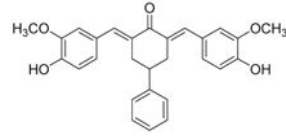**15**, R$_1$ =-OC$_6$H$_5$, R$_2$= -F, R=R$_3$=R$_4$=H
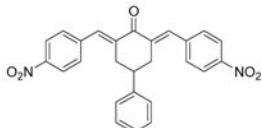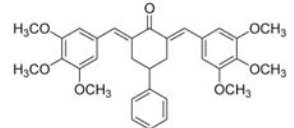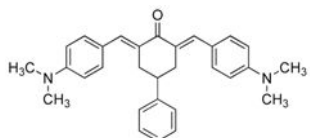
Scheme 1.
Synthesis of the 2,6-bis(benzylidene)-4-phenylcyclohexanones or curcumin analogs **1**–**15**.

Table 1

Cytotoxicity results of synthesized curcumin analogs in B16 and L1210 cell lines as determined by MTT assay.

Compound	IC$_{50}$ (μM)	
	B16	**L1210**
1	15.0 ± 2.8	>100
2	3.4 ± 0.2	3.6 ± 0.4
3	>100	>100
4	12.3 ± 7.7	8.6 ± 3.6
5	3.4 ± 0.5	4.5 ± 1.8
6	3.3 ± 0.3	5.6 ± 0.4
7	3.5 ± 0.3	3.5 ± 0.2

Compound	IC$_{50}$ (μM)	
	B16	L1210
8	1.6 ± 0.6	0.35 ± 0.0
9	0.51 ± 0.1	1.2 ± 0.9
10	Insoluble in DMSO	
11	>100	>100
12	2.1 ± 0.4	2.9 ± 0.6
13	5.3 ± 0.4	4.5 ± 0.5
14	3.2 ± 0.3	3.2 ± 0.3
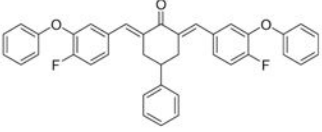
Compound	IC$_{50}$ (μM)	
	B16	**L1210**
15	>100	>100

Table 2

Physical constants of the substituents in analogs **1**–**15**: Hammett σ and Taft σ*, Hansch π, and molar refractivity MR.

Analogs	Substituents	σ/σ*	π	MR
1	4-OCH$_3$	−0.28	−0.02	9.93
2	H	0.00	0.00	3.09
4	3,4-O-CH$_2$-O	−0.27	−0.05	9.99
5	4-Cl	0.24	0.71	8.09
6	4-F	0.06	0.14	2.98
7	3-OCH$_3$	0.11	−0.02	9.93
8	4-NO$_2$	0.78	−0.28	9.42
9	3,4,5-(OCH$_3$)	−0.06	−0.06	23.61
12	3-Br	0.39	0.86	10.94
13	2-Cl	0.37	0.71	8.09
14	3-OCH-3,4-OH	−0.27	−0.69	11.75